Bioorganic & Medicinal Chemistry xxx (2015) xxx–xxx

Contents lists available at ScienceDirect

Bioorganic & Medicinal Chemistry

journal homepage: www.elsevier.com/locate/bmc

Synthesis, anti-mycobacterial activity and DNA sequence-selectivity of a library of biaryl-motifs containing polyamides

Federico Brucoli [a,*], Juan D. Guzman [b,†], Arundhati Maitra [b], Colin H. James [c], Keith R. Fox [d], Sanjib Bhakta [b]

[a] School of Science and Sport, Institute of Biomedical and Environmental Health Research (IBEHR), University of the West of Scotland, Paisley PA1 2BE, UK
[b] Mycobacteria Research Laboratory, Department of Biological Sciences, The Institute of Structural and Molecular Biology, Birkbeck, University of London, London WC1E 7HX, UK
[c] UCL School of Pharmacy, London, 29-39 Brunswick Square, London WC1N 1AX, UK
[d] Centre for Biological Sciences, Life Sciences Building 85, University of Southampton, Southampton SO17 1BJ, UK

ARTICLE INFO

Article history:
Received 30 January 2015
Revised 27 March 2015
Accepted 2 April 2015
Available online xxxx

Keywords:
Distamycin
Antibiotic resistance
Anti-tubercular agents
DNA-minor groove ligands
Whole cell phenotypic evaluation
Combinatorial chemistry

ABSTRACT

The alarming rise of extensively drug-resistant tuberculosis (XDR-TB) strains, compel the development of new molecules with novel modes of action to control this world health emergency. Distamycin analogues containing N-terminal biaryl-motifs **2**(*1-5*)(*1-7*) were synthesised using a solution-phase approach and evaluated for their anti-mycobacterial activity and DNA-sequence selectivity. Thiophene dimer motif-containing polyamide **2**(*2,6*) exhibited 10-fold higher inhibitory activity against *Mycobacterium tuberculosis* compared to distamycin and library member **2**(*5,7*) showed high binding affinity for the 5′-ACATAT-3′ sequence.

1. Introduction

Distamycin (**1**) is a natural product that has long represented a key template for the design of DNA-interactive anti-cancer and anti-infective chemotherapeutic agents.[1,2] **1** is an oligoamidine comprised of three pyrrolo–amido units and one propylamidine chain group, and binds in a non-covalent manner into the DNA-minor groove spanning 4–5 adjacent adenine–thymine (AT) base pairs.[3–5] Distamycin and structurally-derived heterocyclic polyamides, termed lexitropsins, form strong reversible complexes with DNA through a combination of hydrogen bonding to N3 of adenine and O2 of thymines, van der Waals forces and hydrophobic interactions.[6,7] Lexitropsins are in general positively charged, have a crescent-like elongated molecular shape that maintains isohelicity with the DNA helix, and can be programmed to bind to a broad repertoire of DNA sequences.[8,9] DNA minor groove-binding heterocyclic polyamides with high molecular recognition properties have been extensively evaluated for their anticancer activity and studied further as probes for therapeutic intervention against bacterial, fungal, viral, and parasitic infections.[10] For example, early studies demonstrated that distamycin analogues are active in vitro against chloroquine-sensitive and -resistant strains of *Plasmodium falciparum*,[11] and, more recently, it was shown that DNA minor-groove binding ligands exhibited in vitro and in vivo antibacterial activity against multidrug-resistant bacteria[12–14] Moreover, polyamides with branched alkyl chains were found to be active against *Mycobacterium aurum*.[15] However, to our knowledge, evaluation of DNA-minor groove binding agents' activity against *M. tuberculosis* has not been conducted. Tuberculosis is a global threat and in 2013 almost 9 million people contracted this disease in both developing and developed countries.[16,17] Furthermore, the occurrence of extensively-drug resistant TB (XDR-TB) strains demands a prompt therapeutic intervention and, therefore, lead molecules with novel mechanisms of action are urgently needed. Mycobacterial DNA is an attractive target and complete reconstruction of the *M. tuberculosis* regulatory network[18] opened up new avenues for developing anti-tubercular agents with novel mechanisms of action. To this end, sequence-selective DNA minor groove-binding agents can be exploited to target specific promoter regions of *M. tuberculosis* DNA and disrupt transcription factors, causing bacterial cell death and overcoming drug resistance-related issues. To test this hypothesis, we synthesised and evaluated the anti-mycobacterial activity of a 35-member library of distamycin analogues, **2**(*1-5*)(*1-7*), in which the constituent N-terminal pyrrole-formamido moiety of distamycin was substituted with biaryl units in a combinatorial

* Corresponding author. Tel.: +44 (0) 141 848 3624.
E-mail address: federico.brucoli@uws.ac.uk (F. Brucoli).
† Current address: Departamento de Química y Biología, División de Ciencias Básicas, Universidad del Norte, Km 5 vía Puerto Colombia, Barranquilla, Colombia.

http://dx.doi.org/10.1016/j.bmc.2015.04.001
0968-0896/

fashion (Fig. 1). The biaryl-motifs were introduced at the N-terminal position in order to improve the DNA sequence-selectivity of distamycin, and overcome H-bond registry issues relative to polyamides containing repetitive sequences of *N*-methylpyrrole rings, which are thought to be over-curved with respect to the DNA helix.[19] In addition to the anti-mycobacterial activity, we sought to evaluate the effects of the N-terminal biaryl-units on the DNA binding affinity and sequence selectivity of polyamides **2**(*1-5*)(*1-7*). In previous experiments, the inclusion of biaryl-motifs at the C-terminal and middle portion of the distamycin framework, led to polyamides more selective for Guanine–Cytosine(GC)-rich DNA tracts.[20] To this end, we used the ethidium bromide (EtBr) displacement assay to assess the DNA-sequence binding preference (i.e., AT- vs GC-rich sequences) of **2**(*1-5*)(*1-7*). DNase I footprinting was used to identify polyamides' DNA binding sites that could be potential recognition sites for mycobacterial DNA-binding proteins or transcription factors. The polyamides were screened against strains of slow-growing mycobacteria, *Mycobacterium bovis* BCG and *M. tuberculosis* H_{37}Rv and minimum inhibitory concentration values (MIC) were determined. Molecular modelling studies were carried out to elucidate the preferred binding sites of polyamide **2**(*5,7*).

2. Results and discussion

2.1. Chemistry

Polyamides **2**(*1-5*)(*1-7*) were synthesised using a previously developed method,[20] starting from substrate **5**.[21,22] The latter (**5**) was coupled in a parallel fashion with the appropriate bromo-substituted aryl/hetaryl carboxylic acids **3**(*1-5*), using 1-hydroxybenzotriazole (HOBt) and 1,3-diisopropylcarbodiimide (DIC) (Scheme 1).

The resulting five bromo-polyamides **6**(*1-5*) were cross-coupled with boronic acid/esters **4**(*1-7*) using a Pd-catalysed Suzuki–Miyaura protocol, affording polyamides **2**(*1-5*)(*1-7*) in moderate to good yield.

2.2. Whole-cell evaluation and anti-tubercular selectivity

The whole cell evaluation of the polyamides' MIC values, which ranged from 3.9–250 μg/mL, showed that the nature of the biaryl-motifs had a remarkable influence on the inhibitory activity and eukaryotic cell toxicity of **2**(*1-5*)(*1-7*). Table 1 illustrates the most significant results of the anti-tubercular screening, cytotoxicity and the selectivity index (SI). As can be noted, the presence of dithiophene units clearly enhanced the anti-mycobacterial activity, with polyamide **2**(*2,6*) exhibiting approximately 10-fold stronger inhibitory activity (3.9 μg/mL) against *M. tuberculosis* compared to distamycin **1** (31.25 μg/mL). Polyamide **2**(*1,5*) showed inhibitory activity against *M. tuberculosis* at 15.62 μg/mL, whereas the MIC value for both **2**(*1,3*) and **2**(*5,7*) was 31.25 μg/mL. Interestingly, distamycin (**1**) had the same MIC value as **2**(*5,7*) against *M. tuberculosis* and showed the highest inhibitory activity (1.95 μg/mL), amongst **2**(*1-5*)(*1-7*), against *M. bovis*. SI is the ratio between growth inhibition concentration values (GIC_{50} in μg/mL) in macrophages and MIC values in bacteria and indicates the druggability of the inhibitors. **2**(*2,6*) and **2**(*5,7*) exhibited significantly higher SI (16 and 8, respectively) amongst the library members, whilst distamycin had one of the lowest SI (2). The polyamides were moderately cytotoxic towards mouse macrophage RAW264.7 cell lines, with GIC_{50} ranging from 62.5 to 500 μg/mL (Table 1). The polyamides with the highest anti-tubercular specific growth inhibitory activities, **2**(*2,6*) and **2**(*1,5*), both incorporated thiophene dimers in their molecular frameworks. It is anticipated that the lipophilic sulfur atoms in the thiophene rings might enhance the permeability of the polyamides through the highly lipophilic cell-wall of the mycobacteria. Calculation of the polyamides topological molecular polar surface area (TPSA), using the TPSA prediction method devised by Ertl,[23] showed that **2**(*2,6*) and **2**(*1,5*) had TPSA values of 100 and 88 Å, respectively, whereas distamycin had a TPSA value of 179.9 Å. TPSA should be <140 Å for drug-like molecules and our predictions showed that the TPSAs of **2**(*2,6*) and **2**(*1,5*) correlate well with the good transport properties of these polyamides.

2.3. Ethidium bromide assay

Polyamides **2**(*1-5*)(*1-7*) and distamycin **1** were screened against a 512-member hairpin-DNA oligonucleotide library containing all possible (non-degenerate) five base pair sequences, using the ethidium bromide (EtBr) displacement assay.[24] A 1:2 molar ratio of oligonucleotide to ligand was used. The polyamides were found to be adenine-thymine (AT)-selective, binding to the general sequence 5′-AAAWH-3′ (H = C or T or A; W = T or A). One notable exception was represented by **2**(*5,7*), which exhibited a binding preference for the 5′-ACVHA-3′ sequence (V = A or G or C; H = C or T or A). In fact, approximately 25% of the top 30 high-affinity DNA sequences of **2**(*5,7*) were 5′-ACVHA-3′, whereas the same region was not present in the top 25 sites of distamycin. On the other hand, the latter bound with low selectivity and high binding affinity to the whole DNA-hairpin library (Fig. S1b in Supporting information). The distamycin top 30 high-affinity DNA sequences were 5′-WWWXX-3′ (X = any base), thus confirming the ability of the natural product to partially accommodate guanine (G) or cytosine (C) bases at the end of its binding sites.[25]

2.4. DNaseI footprinting

The DNA sequence-selectivity of **2**(*1-5*)(*1-7*) and **1** was further investigated by conducting DNase I footprinting experiments using the 192 base-pair fragment HexB. This fragment contains 31 symmetrical hexanucleotide sequences with a broad range of AT and GC base pair combinations.[26,27] **2**(*1-5*)(*1-7*) generally showed weak interactions with HexB, whereas the thiazole–pyrazole biaryl-motif containing **2**(*5,7*) was found to produce clear footprint areas. The footprinting gel presented in Figure 2 shows the interactions of **2**(*5,7*) and distamycin (dis) with HexB. It should be noted that, although **1** and **2**(*5,7*) protected similar regions within the HexB fragment, clear differences arise in terms of relative concentrations at which the two ligands produce the footprints. Distamycin generated three regions of protection, 5′-TAATTA-3′, 5′-CAATTG-3′ and 5′-TTATAA-3′, at concentrations between 10 and 5 μM, whereas **2**(*5,7*) only produced attenuated cleavage around these sequences, thus suggesting that these sites were not good targets for **2**(*5,7*). Both ligands bound to the 5′-AATATT-3′ and 5′-ATTAAT-3′ sequences, although **2**(*5,7*) with lower binding affinity than distamycin, as can be seen by the attenuated bands of protection within these two sites. More importantly, polyamide **2**(*5,7*) bound with high affinity to the 5′-ACATAT-3′ sequence, which was the central portion of a larger footprinting area, 5′-ATATACATATGTACATG-3′, that is entirely protected by both distamycin and **2**(*5,7*) at higher concentrations. Furthermore, the footprint generated by **2**(*5,7*) at the 5′-ACATAT-3′ site appears to persist to lower concentrations than any of the other footprints produced by this ligand. Although DNase I footprinting cannot identify binding sites with a single-base resolution, it is suggested that the 5′-ACATAT-3′ sequence was **2**(*5,7*) best target within the HexB fragment. The footprinting results confirmed the polyamide selectivity for the 5′-ACVHA-3′ sequence, previously revealed by the EtBr displacement assay, and indicated that substitution of the N-terminal pyrrole-formamido unit of distamycin with the

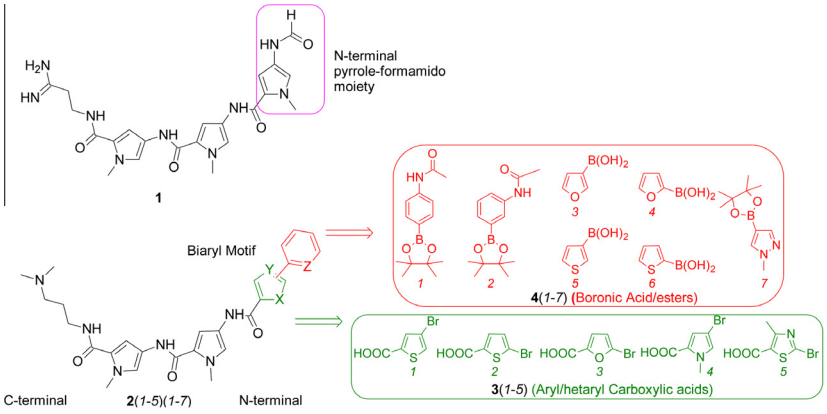

Figure 1. Structures of distamycin (**1**) and polyamides **2**(*1-5*)(*1-7*) with two N-terminal points of diversification attained using building blocks **3**(*1-5*) and **4**(*1-7*).

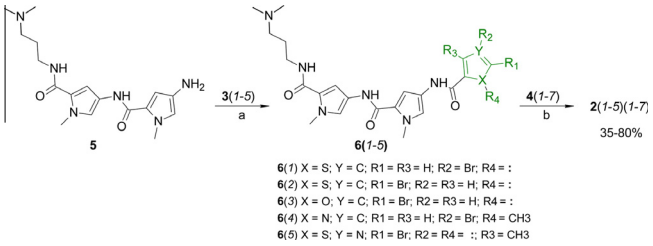

Scheme 1. General synthetic scheme for the preparation of biaryl motifs-including tetra-heterocyclic polyamides library **2**(*1-5*)(*1-7*). (a) **3**(*1-5*), HOBt, DIC, 16 h, rt; (b) **4**(*1-7*), $Pd(PPh_3)_4$, K_2CO_3, microwave.

thiazole–pyrazole biaryl-motif conferred enhanced DNA-sequence affinity and selectivity to polyamide **2**(*5,7*). Biophysical experiments, such as NMR spectroscopy, will be conducted to elucidate the different binding affinities of compound **2**(*5,7*) and distamycin towards the 5′-TAATTA-3′, 5′-CAATTG-3′, 5′-TTATAA-3′, 5′-AATATT-3′ and 5′-ATTAAT-3′ binding sites.

2.5. Molecular modelling

At this stage, in an effort to rationalise the superior DNA-binding affinity and sequence-selectivity of polyamide **2**(*5,7*) for the 5′-ACATAT-3′ site, it was decided to model the interactions of **2**(*5,7*) and distamycin (**1**) with the self-complementary dodecanucleotide $d(G_1C_2A_3C_4A_5T_6A_7T_8G_9T_{10}G_{11}C_{12})_2$ (Fig. 3A and B).

Molecular dynamics simulations (10 ns) of **2**(*5,7*) and **1** bound in the minor groove of the duplex-DNA were carried out in explicit solvent conditions and with one positive formal charge on the ligands' amino- and diamidine-tails. This was followed by free energy calculations in relation to binding of the ligands to the duplex-DNA, as a measure of binding strength. Both directional orientations of **2**(*5,7*) and **1** in the minor groove were modelled, that is, with the C-terminal cationic tails (orientation 1) and with the N-terminal residues at the A3 position of the duplex-DNA (orientation 2). The free energy of binding suggested the preferred orientation of **2**(*5,7*) was with the pyrazole ring at the A3 position of the duplex (orientation 2), whereas for distamycin orientation 1 was the most favoured. It was also found that, for orientation 2, the free energy of binding of **2**(*5,7*) was considerably higher than that of **1**. Figure 3 A shows that **2**(*5,7*) follows the minor groove tract spanning approximately six base pairs. Polyamide **2**(*5,7*) was initially positioned at A3, moving very little throughout the simulation. It is suggested that DNA-duplex stability was afforded by the orientation of the CH of the pyrazole ring positioned between the oxygen atoms of C4 and T22, the hydrogen of the CH group having a slight positive partial charge (Fig. 3B). Similar stability arises from the interactions of the ligand's N-terminal amide NH, positioned between T20:O2 and T6:O2, and the C-terminal amide NH, positioned between A19:N3 and A7:N3. The NH of the N-terminal amide also forms a hydrogen bond to A5:N3.

3. Conclusions

A combinatorial library of novel biaryl-motif-including polyamides **2**(*1-5*)(*1-7*) was synthesised and screened against *M. bovis* BCG and *M. tuberculosis* $H_{37}Rv$. The results revealed that dithiophene-containing polyamide **2**(*2,6*) inhibited the *M. tuberculosis* $H_{37}Rv$ growth at 3.9 μg/mL and had an 8-fold higher selectivity index compared to distamycin. The clinically relevant anti-tubercular potency of **2**(*2,6*) and its improved therapeutic window are encouraging results that can contribute to the development of drug-leads. Furthermore, it was found that the inclusion of biaryl-motifs at the N-terminal of the distamycin framework resulted in polyamides with enhanced AT-sequence selectivity and diminished GC-promiscuity compared to distamycin. In particular, the N-terminal thiazole–pyrazole biaryl-motif conferred enhanced DNA sequence-selectivity, but reduced anti-mycobacterial activity, to compound **2**(*5,7*), which bound with high affinity to the 5′-ACATAT-3′ site within the HexB fragment. Although the strong inhibitory activity of **2**(*2,6*) against the pathogenic *M. tuberculosis* strain does not correlate well with its ability to recognise predetermined DNA-binding sites, the complete AT-sequence selectivity of this polyamide would be desirable. In fact, despite the high GC content of the mycobacteria genome, **2**(*2,6*), or indeed analogues structurally derived from this compound, could modulate and inhibit the activity of mycobacterial transcription factors or proteins regulators, such as Lrs2, which binds to AT-rich DNA sequences and regulates important pathways in antibiotic-induced genes expression in *M. tuberculosis*.[28] In addition, more hydrophobic heterocyclic rings, such as the 2-chlorothiophene ring,[14] could be included in the biaryl-motifs of novel minor groove binders to improve membrane permeability and antibacterial activity. The results presented here show that AT-sequence selective DNA-minor groove binding agents can be further investigated as potential anti-tubercular therapeutic leads.

4. Experimental section

4.1. Chemistry

HPLC analyses were carried out on a Phenomenex Monolithic C_{18} reversed-phase column (50 × 4.6 mm) with a flow rate of 1.5 mL min^{-1} and a linear gradient of 5–95% B over 10 min.

Table 1
Biological activity screening results

Structure	Entry	*M. tuberculosis* $H_{37}Rv$[a]	*M. bovis* BCG[a]	RAW 264.7[b]	SI[c]
Distamycin	**1**	31.25	1.95	62.5	2
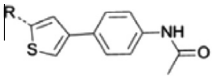	**2**(*1,1*)	62.5	125	62.5	1
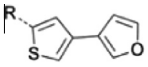	**2**(*1,3*)	31.25	125	250	8
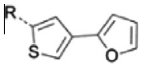	**2**(*1,4*)	250	125	62.5	0.25
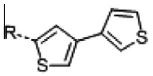	**2**(*1,5*)	15.62	31.25	62.5	4
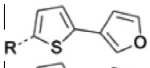	**2**(*2,3*)	62.5	7.8	62.5	1
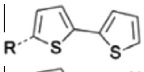	**2**(*2,6*)	3.9	15.6	62.5	16
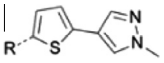	**2**(*2,7*)	250	125	62.5	0.25
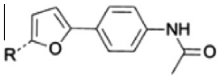	**2**(*3,1*)	125	125	250	2
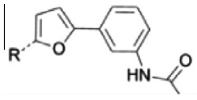	**2**(*3,2*)	125	125	500	4
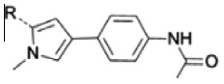	**2**(*4,1*)	125	125	500	4
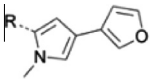	**2**(*4,3*)	62.5	62.5	500	8
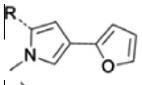	**2**(*4,4*)	62.5	125	500	8
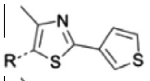	**2**(*5,5*)	250	125	62.5	0.25
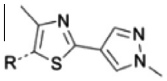	**2**(*5,7*)	31.25	62.5	250	8
Isoniazid	INH	0.05	0.05	3000	60,000
Rifampin	RIF	0.05	0.05	700	14,000

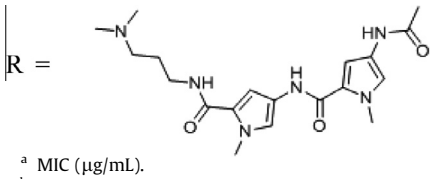

[a] MIC (μg/mL).
[b] GIC_{50} (μg/mL) in RAW264.7 mouse macrophage cell line.
[c] SI = GIC_{50}/MIC.

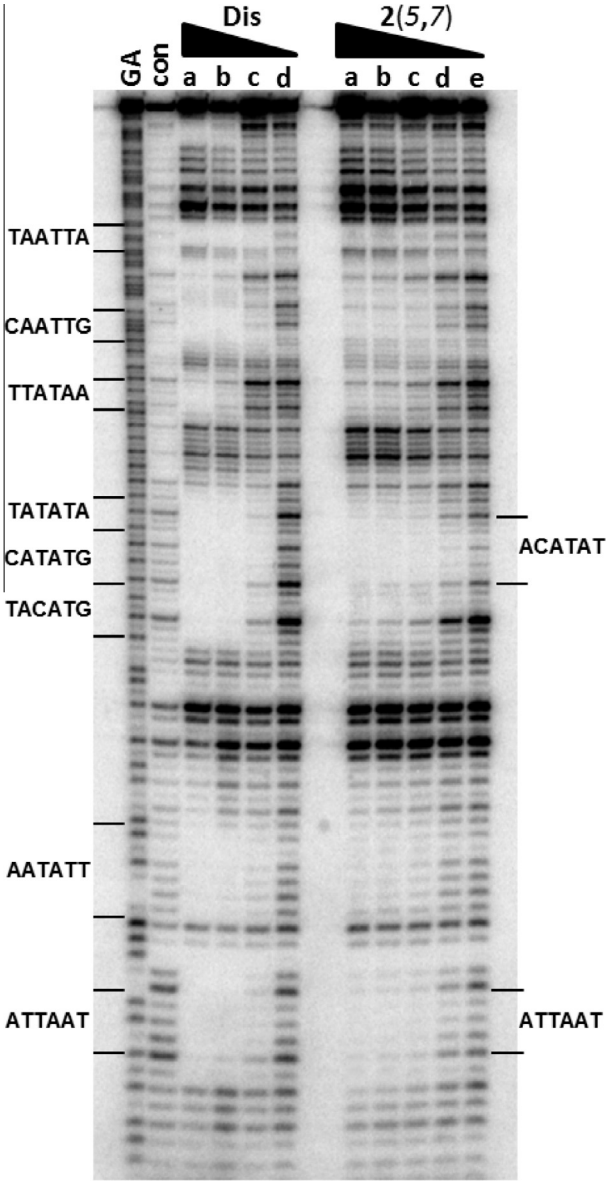

Figure 2. DNase I pattern for HexB fragment in the presence of distamycin (Dis) and **2**(*5,7*). Lanes a, b, c, d and e correspond to concentrations of 10, 7, 5, 3 and 1 μM. Marker lanes labelled 'GA' are specific for purines, and the control lane, 'con', shows digestion of DNA in the absence of ligand.

Eluent A: H_2O/0.1% formic acid; eluent B: CH_3CN/0.1% formic acid. Peak areas were integrated with UV at 250 nm. The LC/MS consisted of a Waters Alliance 2695 HPLC coupled to a Micromass ZQ mass spectrometer using positive electrospray ionization mode (ESI^+). NMR spectra were acquired using a Brucker Advance 400 spectrometer. Chemical shifts are reported in parts per million (ppm) with the solvent resonance as the internal standard and coupling constants (*J*) are quoted in Hertz (Hz). Spin multiplicities are described as: s (singlet), br s (broad singlet), d (doublet), dd (doublet of doublets), t (triplet) and m (multiplet). Data are reported as follows: chemical shift, multiplicity, coupling constant, integration and assignment (py = pyrrole, th = thiophene, fu = furan, thz = thiazole, pz = pyrazole). Microwave assisted chemistry was performed on an Emry's Optimizer Personal Chemistry, Biotage AG. Reaction mixtures of polyamides **2**(*1-5*)(*1-7*) were initially purified using Isolute SCX-2 (silica-based sulfonic acid) cartridges. Final purification was achieved either by conventional column chromatography or by mass directed preparative HPLC using a Waters 2996 PDA detector, Waters 515 HPLC pump and Waters 2525 binary gradient module. Solvents were removed from the purified compounds using a VC3000 Genevac and freeze dried using a Heto Lyolab 3000 freeze drier. High-resolution mass spectra (HRMS) were obtained on a Thermo Navigator mass spectrometer coupled to LC using electrospray ionization (ESI) and time-of-light (TOF) mass spectrometry. Accurate molecular masses were determined using either [Glu]-fibrinopeptide B ($[M+2H]^{2+}$ = 785.8426) or cortisone

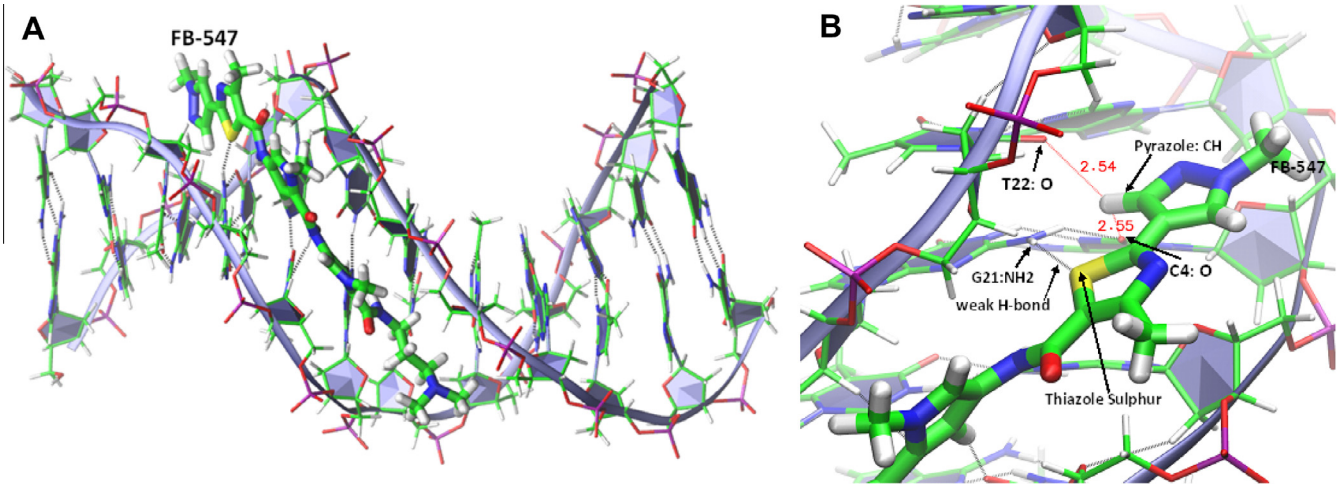

Figure 3. (A) Structure of the complex for **2**(*5,7*) (FB-547) binding to a 12-mer DNA duplex containing an embedded 5′-ACATAT-3′ tract. (B) Detail of the pyrazole-thiazole biaryl unit in relation to residues G21, T22 and C4 of the minor groove. Key: red numerals are distances in Å, black dashed lines are hydrogen bonds.

($[M+H]^+$ = 361.2010) as an internal standard. Chemicals were purchased from Sigma-Aldrich and VWR.

The synthetic procedures for the preparation of intermediate **5** and bromo-polyamides **6**(*1-5*), and the ^{1}H NMR data and High Resolution Mass Spectra (HRMS) for the novel tetra-heterocyclic polyamides are reported in the Supporting information.

General procedure A: amide coupling of dipyrrole platform 5 with bromo-substituted aryl/hetaryl carboxylic acid 3(*1-5*) to give bromo-substituted polyamides 6(*1-5*)

HOBt (2 equiv) and DIC (1.5 equiv) were added to a solution of amine **5** and the appropriate bromo-substituted aryl/hetaryl carboxylic acid **3**(*1-5*) (1.3 equiv) in dry CH_2Cl_2 (10 mL). The reaction mixture was allowed to stir for the required amount of time (see Supporting information). The resulting solution was subsequently passed through a SCX-2 cartridge (sorbent mass $\geqslant$ 10 times of the product mass) and washed with CH_2Cl_2 (3 × 10 mL), DMF (3 × 10 mL) and MeOH (2 × 10 mL). A solution of NH_3 in MeOH (60 mL, 2 M) was then utilised to release the product from the cartridge. After removing the solvent under reduced pressure, the products **6**(*1-5*) were directly utilised as a substrate for the following Suzuki chemistry.

General procedure B: Suzuki cross-coupling reaction of bromopolyamides 6(*1-5*) with boronic acid/esters 4(*1-7*) to give polyamides 2(*1-5*)(*1-7*)

$Pd(PPh_3)_4$ (0.2 equiv) was added under a nitrogen atmosphere to a solution of bromopolyamides **6**(*1-5*) (0.2 mmol), the appropriate boronic acid/ester **4**(*1-7*) (1.2 equiv) and K_2CO_3 (3 equiv) in a mixture of ethanol, toluene and water (1:1:0.2) (2.2 mL) in a 10 mL microwave vial containing a magnetic stirrer. The reaction mixture was sealed in an inert N_2 environment and heated with microwave radiation in an EMRYS™ Optimizer Microwave Station (Personal Chemistry) at 100 °C for the required amount of time (see Supporting information). After LC–MS analysis revealed the absence of starting material, the reaction mixture was passed through an Isolute™ SCX-2 cartridge and washed with CH_2Cl_2 (3 × 10 mL), DMF (3 × 10 mL) and MeOH (2 × 10 mL). Subsequently, a solution of NH_3 in MeOH (60 mL, 2 M) was employed to release the product from the cartridge. After removing MeOH under reduced pressure, the crude mixture was purified using a preparative HPLC coupled to a mass directed fraction collector. Pure fractions were combined and lyophilised to yield the solid product.

4-(2,2′-Bithiophene-5-carboxamido)-*N*-(5-(3-(dimethylamino)propylcarbamoyl)-1-methyl-1*H*-pyrrol-3-yl)-1-methyl-1*H*-pyrrole-2-carboxamide 2(*2,6*)

The reaction was carried out as described for general procedure B using 107 mg of bromo-substituted polyamide **6**(*2*) (0.2 mmol) and 31 mg of boronic acid **4**(*6*). The reaction mixture was irradiated at microwave frequencies for 11 min. A total of 60 mg (55%) of **2**(*2,6*) was obtained as a yellow solid. ^{1}H NMR (DMSO-d_6) (400 MHz) δ 8.22 (s, 1H), 7.86 (d, J = 3.97 Hz, 1H, th), 7.60 (dd, J = 4.78, 1.13 Hz, 1H, th), 7.44 (dd, J = 3.58, 1.13 Hz, 1H, th), 7.37 (d, J = 3.90 Hz, 1H, th), 7.26 (d, J = 1.80 Hz, 1H, py), 7.19 (d, J = 1.80 Hz, 1H, py), 7.14 (dd, J = 5.09, 3.62 Hz, 1H, th), 7.04 (d, J = 1.86 Hz, 1H, py), 6.83 (d, J = 1.85 Hz, 1H, py), 3.87 (s, 3H, N-CH_3-py), 3.80 (s, 3H, N-CH_3-py), 3.22–3.16 (m, 2H, CH_2 aliphatic chain), 2.29 (t, J = 7.04 Hz, 2H, CH_2 aliphatic chain), 2.18 (s, 6H, $N(CH_3)_2$ aliphatic chain), 1.63 (p, J = 7.04 Hz, 2H, CH_2 aliphatic chain). HRMS [M^+] calculated for $C_{26}H_{30}N_6O_3S_2$ m/z 539.1893, found 539.1812.

***N*-(5-(5-(3-(Dimethylamino)propylcarbamoyl)-1-methyl-1*H*-pyrrol-3-ylcarbamoyl)-1-methyl-1*H*-pyrrol-3-yl)-4-methyl-2-(1-methyl-1*H*-pyrazol-4-yl)thiazole-5-carboxamide 2(*5,7*)**

The reaction was carried out as described for general procedure B using 110 mg of bromo-substituted polyamide **6**(*5*) (0.2 mmol) and 50 mg of boronic ester **4**(*7*). The reaction mixture was irradiated at microwave frequencies for 11 min. A total of 54 mg (50%) of **2**(*5,7*) was obtained as a yellow solid. ^{1}H NMR (CH_3OD) (400 MHz) δ 8.53 (s, 1H, NH-amide), 8.19 (s, 1H, pz), 7.96 (s, 1H, pz), 7.23 (d, J = 1.75 Hz, 1H, py), 7.17 (d, J = 1.79 Hz, 1H, py), 6.98 (d, J = 1.84 Hz, 1H, py), 6.87 (d, J = 1.85 Hz, 1H, py), 3.96 (s, 3H, N-CH_3-pz), 3.92 (s, 3H, N-CH_3-py), 3.89 (s, 3H, N-CH_3-py), 3.39 (t, J = 6.49 Hz, 2H, CH_2 aliphatic chain), 3.02 (t, J = 7.71 Hz, 2H, CH_2 aliphatic chain), 2.79 (s, 6H, –$N(CH_3)_2$), 2.65 (s, 3H, CH_3-thz), 1.95 (p, J = 7.09 Hz, 2H, CH_2 aliphatic chain). ^{13}C NMR (CH_3OD) (100 MHz) δ 162.4, 161.8, 161.0, 160.7, 153.1, 143.0, 138.7, 131.4, 128.3, 126.1, 123.5, 120.1, 102.7, 57.0, 43.9, 39.3, 36.8, 26.8, 16.3. MS m/z (ES+) (relative intensity) 551 ($M^{+\cdot}$). HRMS [M^+] calculated for $C_{26}H_{33}N_9O_3S$ m/z 552.2500, found 552.2481.

4.2. Anti-mycobacterial screening using HT-SPOTi

M. bovis BCG and *M. tuberculosis* H37Rv were grown in Middlebrook 7H9 broth supplemented with 0.02% (v/v) glycerol, 0.05% (v/v) Tween-80 and 10% oleic acid, albumin, dextrose and

catalase (OADC; BD Biosciences) as a rolling culture at 2 rpm and as a stand culture at 37 °C. The antimycobacterial activities of the compounds were tested following the HT-SPOTi.[29] The high throughput growth inhibition assay was conducted in a semi-automated 96 well plate format. Briefly, compounds dissolved in DMSO at a final concentration of 50 mg/ml were serially diluted and dispensed in a volume of 2 μL into each well of a 96 well plate to which 200 μL of Middlebrook 7H10 agar medium kept at 55 °C supplemented with 0.05% (v/v) glycerol and 10% (v/v) OADC was added. A well with no compounds (DMSO only) and isoniazid were used as experimental controls. To all the plates, a drop (2 μL) of mycobacterial culture containing 2×10^3 colony-forming units (CFUs) was spotted in the middle of each well and the plates were incubated at 37 °C for 7 days. The minimum inhibitory concentrations (MICs) were determined as the lowest concentrations of the compound where no mycobacterial growth was directly observed.

4.3. Quantitation of eukaryotic cell toxicity using resazurin assay

The mouse macrophage cell line (RAW264.7) were used for the cytotoxicity assay.[29] Growth inhibitory concentrations (GIC_{50}) were determined by interpolation based on the 50% viability compared to control experiments. Selectivity index (SI) values were calculated as a ratio of GIC_{50} and the MIC values from *M. tuberculosis*.

4.4. Ethidium bromide displacement assay

DNA hairpin oligonucleotides were purchased from Genebase Inc. (San Diego) as 1000 μM (base pairs) solutions in water and stored as stock solutions at −50 °C. Prior to use, each oligonucleotide was diluted to 10 μM in water and stored at 0 °C for no longer than 2 days. Each well of a Costar® 96-well plate (360 μL, black, flat-bottom) was loaded with one hairpin oligonucleotide (5 μL, 1 μM DNA base pairs final concentration) and with ethidium bromide solution containing tris buffer (44 μL, Tris–HCl 0.1 M, NaCl 0.1 M, pH 8, 4.4 μM ethidium bromide final concentration). After 15 min of incubation at room temperature a first reading of fluorescence was carried out using a fluorescent plate reader (EnVision™ multilabel plate reader). EnVision™ plate reader was set up to excite the samples at 545 nm and read the emission at 595 nm. Subsequently, distamycin or a single aliquots of each library member (1 μL of a 0.1 mM solution in DMSO, 2 μM drug final concentration) was added to each well containing the premixed ethidium bromide/DNA oligonucleotide solution. After incubation at room temperature for 45 min, each well was read a second time on the fluorescent plate reader in triplicate experiments with two control wells (no distamycin-no drug = 100% fluorescence, no DNA = 0% fluorescence). The reduction in fluorescence was deduced by comparing the first fluorescence reading with the second one. Fluorescence readings are reported as reduction in fluorescence (%) relative to the controls.

4.5. DNase I footprinting experiments

DNA fragment HexB was prepared according to previously published methods.[27] The radio-labelled DNA was eluted from the gel and dissolved in 10 mM Tris–HCl (pH 7.5) containing 1 mM ethylenediaminetetraacetic acid (EDTA) at a concentration of 10 to 20 counts per second per microliter (cps/μL) as determined with a handheld Geiger counter. GA markers were prepared by mixing 1.5 μL labelled DNA with 20 μL of sterile water and 4 μL DNase I stop solution (10 mM EDTA, 1 mM NaOH, 0.1% bromophenol blue and 80% formamide). The sample was then incubated at 100 °C for about 30 min with the micro-centrifuge tube kept open to allow evaporation, then crash cooled on ice. A control lane was created by combining 1.5 μL of template DNA with 3 μL of buffer (10 mM Tris–HCl at pH 7.5 containing 0.1 mM EDTA). DNase I footprinting was performed mixing 1.5 μL radiolabelled DNA (dissolved in 10 mM Tris–HCl, pH 7.5 containing 0.1 mM EDTA) with 1.5 μL ligand (dissolved in 10 mM Tris–HCl, pH 7.5 containing 10 mM NaCl). The mixture was allowed to equilibrate for 30 min at room temperature before digestion with 2 μL DNase I (dissolved in 20 mM NaCl, 2 mM $MgCl_2$, 2 mM $MnCl_2$). The reaction was stopped after 1 min and the samples were heated at 100 °C for 3 min and crash-cooled on ice. The products were resolved on 8% (w/v) denaturing polyacrylamide gels (40 cm long and 0.3 cm thick). After electrophoresis the gels (1500 V, between 1.5 and 2 h) were fixed (10% acetic acid), dried under vacuum and exposed to a Phosphorimager screen (Molecular Dynamics Storm 860 Phosphorimager).

4.6. Molecular modelling

The ligand **2**(*5,7*) was built and an initial minimization carried out using the ChemBioOffice package. AMBER software was then used to assign partial charges to the ligand using the Am1bcc charge strategy by means of the *antechamber* software, missing parameters being assigned with *parmchk*. Standard B-form duplex DNA was constructed with the AMBER *nab* software. Xleap was used to establish an initial graphical alignment of **2**(*5,7*) in the minor groove, placing the head of the ligand, in each orientation, over residue A3. Initial coordinates and topology file were established with the use of the ff99bsc0 nucleic acid force field parameters along with the *gaff* parameters for the ligand. Prior to creating this, 22 Na+ counter ions were automatically positioned and a 10 Å truncated octahedral periodic water solvent (TIP3P) box created. Initial minimization of the water was carried out, while restraining the DNA and ligand with a high force constant, followed by relaxation of the whole system without restraints. Dynamics (PMEMD) heating, with a periodic boundary, from 0 K to 300 K was then applied over 30 ps at constant volume with the Langevin thermostat in operation (collision frequency of 1.0 ps^{-1}) and mild restraints applied to the DNA and ligand. Further equilibration at 300 K was then applied over 100 ps at constant pressure with no restraints in place. The final dynamics production run was carried out at constant volume at 300 K (NVT) over 10 ns. Throughout dynamics, a time step of 2 fs was used with the SHAKE algorithm applied to bonds involving hydrogen atoms. Amber v11 and AmberTools v1.5 were used. Dynamics was visualized with VMD[309] software.[30] Free energy calculations were performed using the AMBER MM-PBSA approach using constructs generated from the explicit solvent simulations (solvent removed). Of the 5000 frames saved during the 10 ns dynamics, 100 equally spaced frames were used for the free energy calculations, the average free energy being calculated.

Acknowledgements

Professor S. Croft is thanked for granting access to a Containment Level III Lab at the London School of Hygiene and Tropical Medicine, University of London. Professor J. A. Hartley at the Cancer Research UK Drug–DNA Interactions Research Group, UCL Cancer Institute, is thanked for his professional and technical support with the Ethidium Bromide assay.

Supplementary data

Supplementary data associated with this article can be found, in the online version, at http://dx.doi.org/10.1016/j.bmc.2015.04.001.

References and notes

1. Baraldi, P. G.; Bovero, A.; Fruttarolo, F.; Preti, D.; Tabrizi, M. A.; Pavani, M. G.; Romagnoli, R. *Med. Res. Rev.* **2004**, *24*, 475.
2. Cortesi, R.; Esposito, E. *Mini-Rev. Med. Chem.* **2010**, *10*, 217.
3. Chen, F. M.; Sha, F. *Biochemistry* **1998**, *37*, 11143.
4. Lah, J.; Vesnaver, G. *Biochemistry* **2000**, *39*, 9317.
5. Asagi, M.; Toyama, A.; Takeuchi, H. *Biophys. Chem.* **2010**, *149*, 34.
6. Dervan, P. B. *Bioorg. Med. Chem.* **2001**, *9*, 2215.
7. Dervan, P. B.; Doss, R. M.; Marques, M. A. *Curr. Med. Chem. Anticancer Agents* **2005**, *5*, 373.
8. Chenoweth, D. M.; Dervan, P. B. *J. Am. Chem. Soc.* **2010**, *132*, 14521.
9. Anthony, N. G.; Johnston, B. F.; Khalaf, A. I.; MacKay, S. P.; Parkinson, J. A.; Suckling, C. J.; Waigh, R. D. *J. Am. Chem. Soc.* **2004**, *126*, 11338.
10. Barrett, M. P.; Gemmell, C. G.; Suckling, C. J. *Pharmacol. Ther.* **2013**, *139*, 12.
11. Lombardi, P.; Crisanti, A. *Pharmacol. Ther.* **1997**, *76*, 125.
12. Khalaf, A. I.; Bourdin, C.; Breen, D.; Donoghue, G.; Scott, F. J.; Suckling, C. J.; MacMillan, D.; Clements, C.; Fox, K.; Sekibo, D. A. T. *Eur. J. Med. Chem.* **2012**, *56*, 39.
13. Anthony, N. G.; Breen, D.; Clarke, J.; Donoghue, G.; Drummond, A. J.; Ellis, E. M.; Gemmell, C. G.; Helesbeux, J.-J.; Hunter, I. S.; Khalaf, A. I.; Mackay, S. P.; Parkinson, J. A.; Suckling, C. J.; Waigh, R. D. *J. Med. Chem.* **2007**, *50*, 6116.
14. Kaizerman, J. A.; Gross, M. I.; Ge, Y.; White, S.; Hu, W.; Duan, J.-X.; Baird, E. E.; Johnson, K. W.; Tanaka, R. D.; Moser, H. E.; Bürli, R. W. *J. Med. Chem.* **2003**, *46*, 3914.
15. Khalaf, A. I.; Anthony, N.; Breen, D.; Donoghue, G.; Mackay, S. P.; Scott, F. J.; Suckling, C. J. *Eur. J. Med. Chem.* **2011**, *46*, 5343.
16. WHO. *Global tuberculosis report 2012*. Geneva: WHO.
17. Guzman, J. D.; Gupta, A.; Bucar, F.; Gibbons, S.; Bhakta, S. *Front. Biosci.* **2012**, *17*, 1861.
18. Galagan, J. E.; Minch, K.; Peterson, M.; Lyubetskaya, A.; Azizi, E.; Sweet, L.; Gomes, A.; Rustad, T.; Dolganov, G.; Glotova, I.; Abeel, T.; Mahwinney, C.; Kennedy, A. D.; Allard, R.; Brabant, W.; Krueger, A.; Jaini, S.; Honda, B.; Yu, W.-H.; Hickey, M. J.; Zucker, J.; Garay, C.; Weiner, B.; Sisk, P.; Stolte, C.; Winkler, J. K.; Van de Peer, Y.; Iazzetti, P.; Camacho, D.; Dreyfuss, J.; Liu, Y.; Dorhoi, A.; Mollenkopf, H.-J.; Drogaris, P.; Lamontagne, J.; Zhou, Y.; Piquenot, J.; Park, S. T.; Raman, S.; Kaufmann, S. H. E.; Mohney, R. P.; Chelsky, D.; Moody, D. B.; Sherman, D. R.; Schoolnik, G. K. *Nature* **2013**, *499*, 178.
19. Kelly, J. J.; Baird, E. E.; Dervan, P. B. *Proc. Natl. Acad. Sci. U.S.A.* **1996**, *93*, 6981.
20. Rahman, K. M.; Reszka, A. P.; Gunaratnam, M.; Haider, S. M.; Howard, P. W.; Fox, K. R.; Neidle, S.; Thurston, D. E. *Chem. Commun.* **2009**, 4097.
21. Chavda, S.; Babu, B.; Patil, P.; Plaunt, A.; Ferguson, A.; Lee, M.; Tzou, S.; Sjoholm, R.; Rice, T.; Mackay, H.; Ramos, J.; Wang, S.; Lin, S.; Kiakos, K.; Wilson, W. D.; Hartley, J. A.; Lee, M. *Bioorg. Med. Chem.* **2013**, *21*, 3907.
22. Kumar, R.; Lown, J. W. *Org. Biomol. Chem.* **2003**, *1*, 2630.
23. Ertl, P.; Rohde, B.; Selzer, P. *J. Med. Chem.* **2000**, *43*, 3714.
24. Rahman, K. M.; Jackson, P. J.; James, C. H.; Basu, B. P.; Hartley, J. A.; de la Fuente, M.; Schatzlein, A.; Robson, M.; Pedley, R. B.; Pepper, C.; Fox, K. R.; Howard, P. W.; Thurston, D. E. *J. Med. Chem.* **2013**, *56*, 2911.
25. Luck, G.; Zimmer, C.; Reinert, K. E.; Arcamone, F. *Nucleic Acids Res.* **1977**, *4*, 2655.
26. Hampshire, A. J.; Fox, K. R. *Anal. Biochem.* **2008**, *374*, 298.
27. Hampshire, A. J.; Rusling, D. A.; Broughton-Head, V. J.; Fox, K. R. *Methods* **2007**, *42*, 128.
28. Gordon, B. R. G.; Li, Y.; Wang, L.; Sintsova, A.; van Bakel, H.; Tian, S.; Navarre, W. W.; Xia, B.; Liu, J. *Proc. Natl. Acad. Sci. U.S.A.* **2010**, *107*, 5154.
29. (a) Guzman, J. D.; Evangelopoulos, D.; Gupta, A.; Birchall, K.; Mwaigwisya, S.; Saxty, B.; McHugh, T. D.; Gibbons, S.; Malkinson, J.; Bhakta, S. *BMJ Open* **2013**, *3*; (b) Guzman, J. D.; Pesnot, T.; Barrera, D. A.; Davies, H. M.; McMahon, E.; Evangelopoulos, D.; Mortazavi, P. N.; Munshi, T.; Maitra, A.; Lamming, E. D.; Angell, R.; Gershater, M. C.; Redmond, J. M.; Needham, D.; Ward, J. M.; Cuca, L. E.; Hailes, H. C.; Bhakta, S. *J. Antimicrob. Chemother.* **2015** [Epub ahead of print].
30. Humphrey, W.; Dalke, A.; Schulten, K. *J. Mol. Graphics* **1996**, *14*, 33.